Sigma Journal of Engineering and Natural Sciences, Vol. 42, No. 6, pp. XX-XX, December, 2024
Yildiz Technical University Press, Istanbul, Turkey

A comparative study on the machining performance of eco-friendly low-lead and lead-free brass alloys in replacement for leaded ones

Nima ZOGHIPOUR[1,2,*], Emre TAŞCIOĞLU[1], Ali Özkan KESKİN[2], Yusuf KAYNAK[2]

ABSTRACT

The use of brass alloys in pipelines and other fluid-carrying systems is widely recognized. The rolled or extruded bars are often machined to produce the manufactured products from these materials. When incredible machinability is required, leaded brasses are frequently employed. Leaded brass usage is prohibited, nevertheless, in systems that deal with environmental and human health hazards. In this study, three types of available brasses in EUA7038 (Brass for European Potable Water Applications List) leaded (CW617N), low-leaded (CW511L) and lead-free (CW724R) brasses haves been taken into consideration in terms of machinability; cutting forces, entry and exit burr height, subsurface microhardness, and microstructures. Experiments have been performed using several levels of feed and cutting speed on the mentioned materials during drilling tests. According to the obtained results, compared to leaded brass materials, low-leaded and lead-free brass materials showed more subsurface deformation. CW511L displays a sharper amendment rate of the in both entry and exit burr height with an increase in feed compared to CW724R and CW617N. It is significant to note that the machinability values for CW511L, CW724R, and CW617N are 1.4, 1.8, and 1.95 times, respectively.

Keywords: *Brass; Lead; Machining; Surface Integrity; Twinning*

INTRODUCTION

Brass is an appealing material for a variety of industrial applications due to its combination of strong corrosion resistance, adequate endurance against wear, high thermal and electric conductivity, and formability. Different types of brass materials are being exposed to machining procedures before being utilized to manufacture components for drinking water delivery systems. Lead element is frequently added to the chemical composition of brass materials in order to improve the machinability for their use in plumbing and bearings [1]. Due to lead's poor solubility in copper alloys, the microstructure of the material contains distributed globules of lead. Lead acts as a lubricant, which reduces the coefficient of friction between the tool and the material, reduces the cutting force and the rate of tool wear, and produces discontinuities that encourage chip fragmentation [2–9]. But because lead is poisonous, its use has given rise to new worries about risks to both human health and the environment. New standards [10–11] are being issued as a result, based on the allowable lead concentration in drinking water systems. By adding other elements, brass alloys' machinability properties have improved. For instance, SeBiLLOYS (Se/Bi alloys) are as machinable as leaded brasses, but Bi is scarce and costs nearly 10 times as much as lead [12,13]. Additionally, a rise in Bi causes copper and copper alloys to become more brittle [13].

Lead- and lead-free brass turned samples' surface topography was studied by Reddy et al. [14]. They used a generic statistical approach to confirm the results and numerically assess the sample's surface topography. Their findings show that turned samples of lead brass had rougher surfaces than lead free brass. Toulfatzis et al. [15] tested the turning machinability of three lead-free brass alloys, CuZn42 (CW510L), CuZn38As (CW511L), and CuZn36 (C27450), in contrast to a reference free-cutting leaded brass CuZn39Pb3 (CW614N). Using the Taguchi approach, they compared quality attributes including cutting force and surface roughness. By applying heat treatments to lead-free brass alloys (CuZn42, CuZn38As and CuZn36), they modified the microstructure and increased the β-phase

This paper was recommended for publication in revised form by Regional Editor Ahmet Selim Dalkilic
[1] Torun Metal Alaşımları Metal Sanayi ve Ticaret A.Ş., GOSB İhsan Dede Caddesi No: 116 41480 Gebze,Kocaeli, Turkey
[2] Department of Mechanical Engineering, Marmara University, 34722 Goztepe Campus-Istanbul
** E-mail address: nima.zoghipour@gmail.com*
Orcid id: https://orcid.org/ 0000-0002-5374-923X Nima Zoghipour, 0000-0001-8913-5304 Emre Taşçıoğlu, 0000-0003-3540-4323 Ali Özkan Keskin, 0000-0003-4802-9796 Yusuf Kaynak
Manuscript Received 07 August 2023, Revised 23 September 2023, Accepted 08 October 2023

content, creating a potential foundation for enhanced chip breakability and improved machinability in other work [16]. Aytekin [17] has conducted a thorough investigation to describe the machinability of lead-free brass alloys. Based on analyses of the cutting force and chip production, their work has mainly concentrated on turning and drilling operations. They also looked at how tool geometry affects machinability, and their findings showed that turning lead-free alloys generates much larger cutting forces than turning leaded alloys. Tam et al. [18] used face turning experiments to assess the machinability of lead-free and free machining brasses in light of cutting forces and machining residual stresses. In order to assess the machinability of prepared and reference materials, Özbey [19] concentrated on the surface roughness and chip formation. His findings showed that the sample made with both MoS2 and MnS additions produced chips of the discontinuous kind. Due to the varied morphologies of the Widmanstäetten, dendritic, and coarse grains, the microstructure of lead-free brass alloys may be divided into three categories based on the kind, amount, and solidification parameter of the additives. Furthermore, depending on the distribution of phases, increasing beta phase in the microstructure also increased the hardness value. CuZn21Si3P's machinability was assessed by Schultheiss et al. [20] in comparison to other widely used, lead-containing free-machining brasses. Their findings revealed that CuZn21Si3P's machinability had significantly decreased. After 142 minutes of machining, CuZn21Si3P, which had been substantially fixed by a coating on the cutting tool, failed when turned lengthwise. Johansson et al. [21] focused on burr formation, differences in cutting pressures, and cutting resistance to compare the machinability of a conventional free-machining leaded alloy with brass alloys with reduced lead concentration. Their findings indicate that alloys with less lead do not exhibit as good machinability as leaded brass. During external turning, Nobel et al. [22] examined the impact of microstructure and silicon as an alloying element, in addition to several tool coatings such TiB2, DLC, and diamond, on chip formation, cutting forces, tool temperatures, and tool wear. Using two distinct types of drilling equipment, Zoghipour et al. [23-24] investigated the impact of the drilling process on the surface integrity properties of lead-free brass alloy. They demonstrated that cutting tools have a significant impact on both the surface and subsurface hardening of lead-free alloys as well as deformation twinning. By modifying tool geometry taking into account web thinning, the helix angle, and the chip morphology, Kato et al. [25] enhanced the chip evacuation in CuZn21Si3P micro-drilling. Fountas et al. [26] focused their inquiry into the machinability of the CuZn39Pb3 brass alloy on the impact of the cutting conditions on the primary cutting force and the surface roughness parameters Ra and Rt.

Only a few studies have been focused on the machinability of new developed brass alloys which are allowed for drinking water in literature. In this study, the ability to be machined of three distinct types of brasses—leaded (CW617N), low-leaded (CW511L), and without lead (CW724R) brasses—has been examined. These brasses were examined in terms of their cutting abilities, entrance and exit burr heights, subsurface microhardness, and microstructures. Several levels of feed and cutting speed have been tested on the relevant materials during penetration testing.

MATERIAL AND METHODS

WORK MATERIALS

Figure 1. The three distinct brass alloys employed in this study's workpieces were lead-free CuZn21Si3P (CW724R), low-leaded CuZn38As (CW511L), and lead-free CuZn40Pb2 (CW617N), all of which were hot extruded round bars with 60 X 50 mm. Table 1 illustrates the mechanical characteristics and elemental composition of the test materials. The restriction of the Pb element is obvious form the chemical composition. Figure 1 depicts the microstructural of the described materials. The dual phase nature of CW617N and CW511L is evident. But CW724R is consisting of three phases. The light yellow, light brown areas represent α and β phases. κ and γ phases are appeared in CW724R structure.

Table 1. The studied brass alloys' chemical composition [27]

	E, GPa	Machinability, %	Composition	Cu	Zn	Pb	Sn	Fe	Ni	Al	As	Mn	P	Si
CuZn40Pb2 (CW617N)	96	95	%Min.	57.0	Rem.	1.6	-	-	-	-	-	-		-
			%Max.	59.0	Rem.	2.5	0.3	0.3	0.3	0.05	-	-	-	-
CuZn38As (CW511L)	100	40	%Min.	61.5	Rem.	-	-	-	-	-	0.02	-	-	-
			%Max.	63.5	Rem.	0.2	0.1	0.1	0.3	0.05	0.15	-	-	-
CuZn21Si3P (CW724R)	100	80	%Min.	75.0	Rem.	-	-	-	-	-	-	-	0.02	2.7
			%Max.	77.0	Rem.	0.09	0.3	0.3	0.2	0.05	-	0.05	0.10	3.5

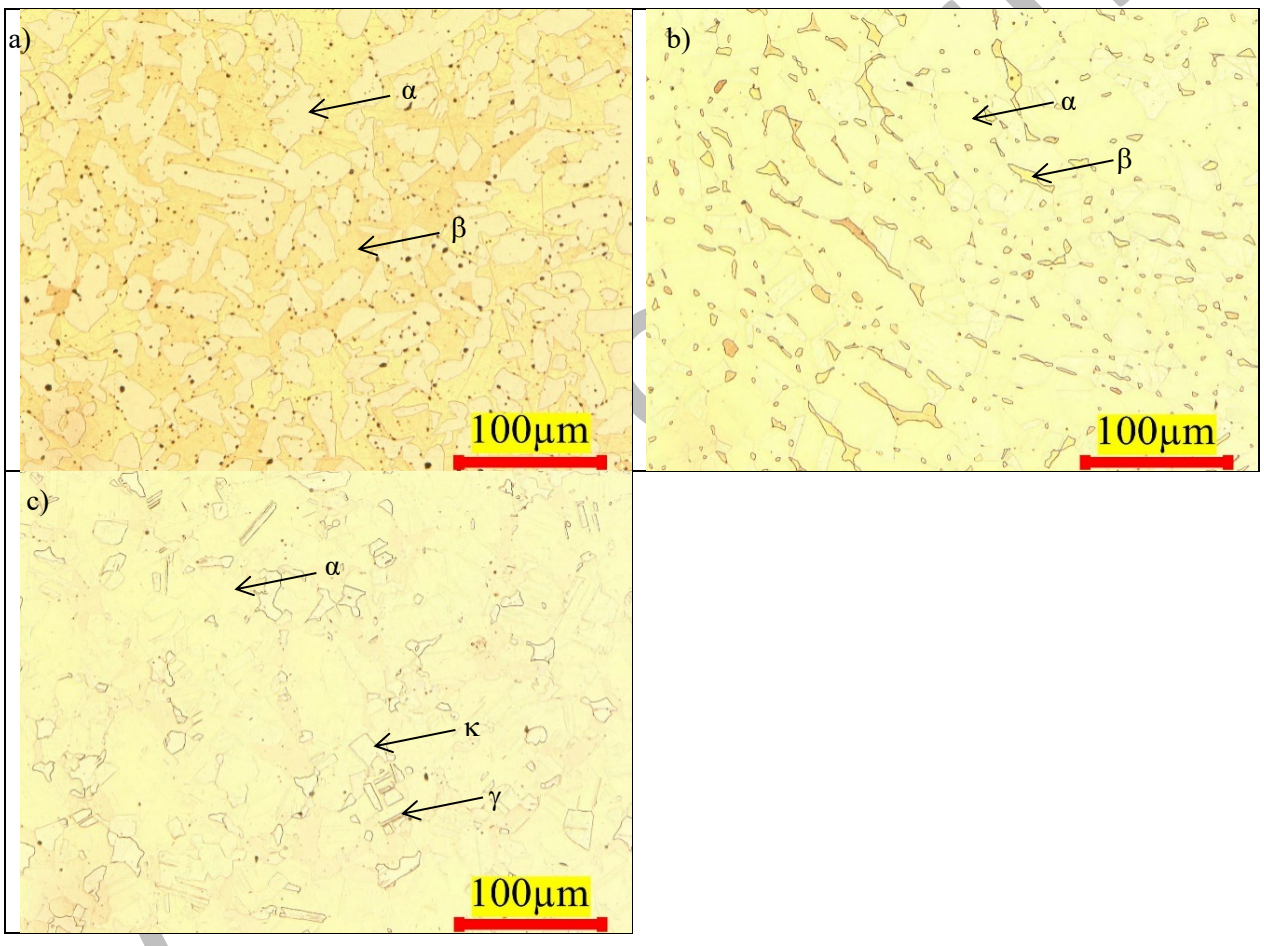

Figure 1. The microstructure of the investigated materials; a) CW617N, b) CW511L, c) CW724R.

EXPERIMENTS AND MEASUREMENTS

Fanuc Robodrill α-D21LiB5 CNC milling was used for the machining experiments. The drill utilized in the studies had a 12 mm diameter, a 30° helix angle, a 6° radial rake angle, and an edge radius of 19 µm. Internal cooling liquid was used to control the feed while maintaining the cutting speed at 120 m/min while drilling through holes at 0.05, 0.1, and 0.15 mm/rev. The samples were etched for about 20 seconds at room temperature using an aqueous

solution of 30 mL of water, 3.5 mL of hydrogen peroxide, and 4.25 g of (NH4)2S2O8, after which the samples were rinsed with deionized water and ethanol and dried once more. SEM (Scanning electron microscopy) and Keyence digital optic microscope were used to analyze surface and sub-surface alterations as well as burr development at the entry and exit of the machined holes. As shown in Fig. 2a, the formation of a burr and in Figure 2b, c the size measurements were made at an angle of one quarter of the diameter is illustrated. The average result of ten measurements from micro-hardness tests with an applied force of 25 g are presented. The cutting forces were measured using a Kistler dynamometer. The used experimental setup is demonstrated in Figure 3.

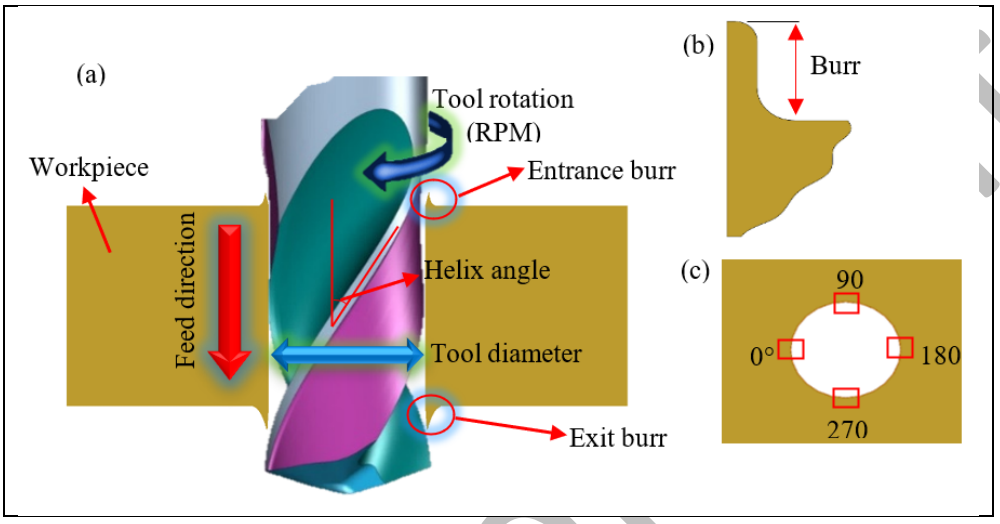

Figure 2. Burr profile displaying (a) how burrs form during drilling (b) a thorough explanation of burr height (c) burr height measuring locations.

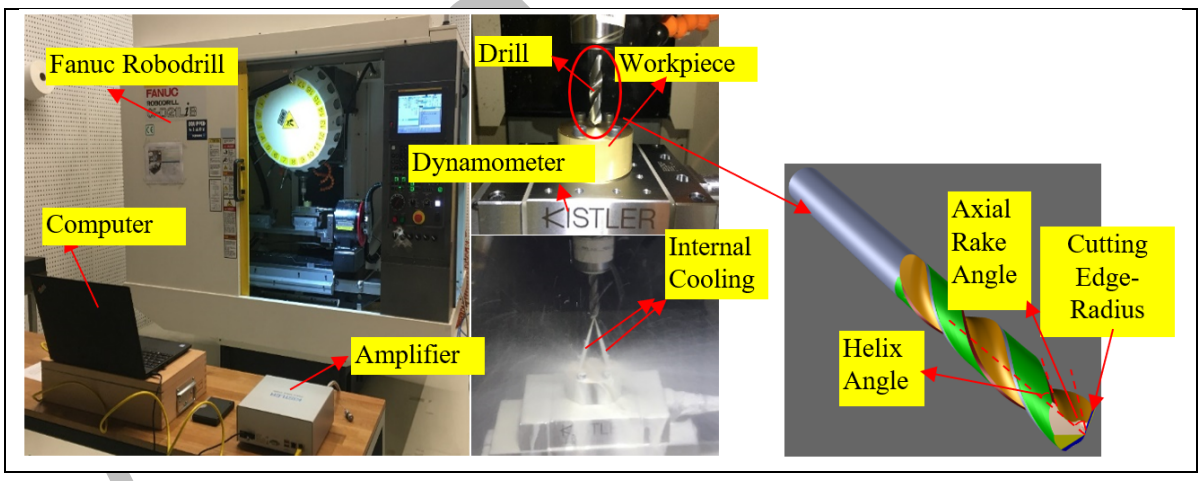

Figure 3. The experimental setup in this study.

RESULTS AND DISCUSSIONS

CUTTING FORCES MEASUREMENTS

An in-depth understanding of the drilling operations' burr development and acquired hole quality requires evaluation of the cutting forces and torques. Figure 4 displays the measured feed force values with relation to feed rate

for three different types of brass alloys. The highest feed force measured was roughly 902 N for CW511L at 0.15 mm/rev, however for CW724R and CW617N, it was 483 N and 345 N, respectively. At 0.05 mm/rev of feed, the minimum values of feed force were measured as 421 N, 259 N, and 204 N for CW511L, CW724R, and CW617N, respectively. With the increase in feed and decrease in the amount of Lead element in the chemical composition, it is clear that the feed forces have been enhanced. The boost in the contact area is mostly responsible for this intensification in the measured value. Despite having more Pb than CW724R, CW511 has a faster rate of feed force growth. This significant variation in observed feed force can be attributable to the presence of Si and P components in CW724R, which improves the machinability and is consistent with results from [20-24-25]. Because of the characteristics of Pb that were described in the first portion of this study, the leaded brass, CW617N, has shown the least cutting forces. It is obvious that the feed forces have increased due to the rise in feed and decrease in the quantity of Lead element in the chemical composition. This intensification in the measured value is mostly caused by the increase in the contact area [23].

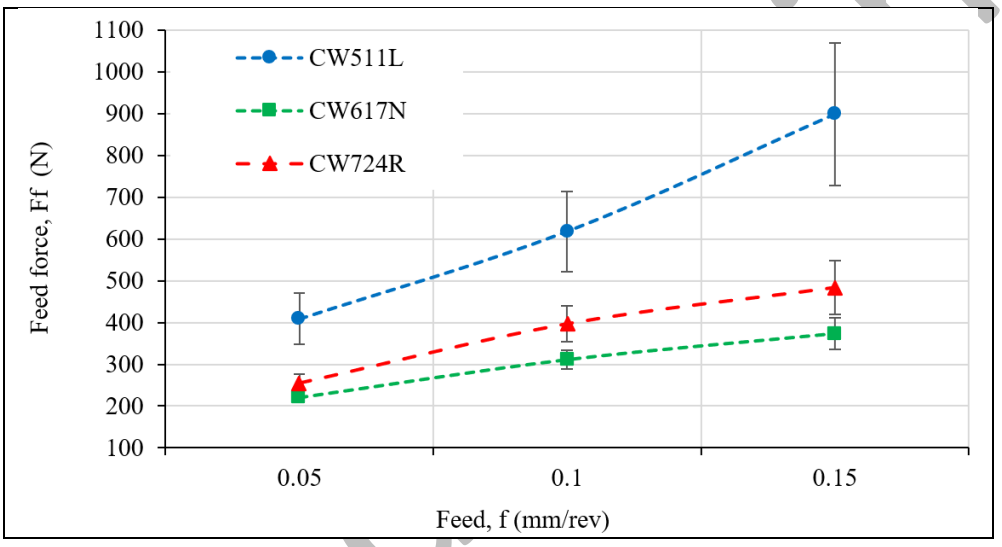

Figure 4. The measured feed forces in this study.

SURFACE AND SUB-SURFACE MICROHARDNESS MEASUREMENTS

One of the outstanding properties of metallic materials is their capacity to respond to different environmental conditions, such as corrosive, frictional, and contact ones. This property is known as surface and sub-surface microhardness. The microhardness of the CW511L, CW617N, and CW724R as received was determined to be 122, 93, and 88 HV, respectively. From the drilled surfaces, depths of 15, 25, 50, 75, 150, 300, and 500 µm were used to determine the microhardness. Figure 5 demonstrates the results of microhardness tests performed on machined experiment samples at various feeds and depths from the surface. Following the use of machining methods, the hardness of the machined samples significantly improved in comparison to the raw samples. For CW724R at 0.15 mm/rev of feed rate, the maximum sub-surface has been recorded at 197 HV on 15 µm depth of the surface. For CW511L and CW617N, these values were measured as 172 and 129 HV, respectively. The highest sub-surface micro hardness values were 173, 107, and 90 HV at a feed of 0.05 mm/rev. It is clear that for CW724R, CW511L, and CW617N, respectively, the hardness at the maximum feed has improved by 61.4%, 84.9%, and 46.5% in comparison to the surface that has not undergone a drilling operation. It is obvious that hardening happens under all adverse circumstances, showing that the cutting tool movement caused severe strain hardening to be conducted via plastic deformation on the substance's surface [24]. In Figure 5, the area where strain hardening has taken place is indicated. In addition, when feed is increased, the hardness of the machined surface increases due to the increased contact area between the cutting tool and the workpiece and the resulting friction on the rake face of the tool and material. The

affected sub-surface elevated by strain hardening is significantly more striking since it is closer to the surface and is located at lower depths [25].

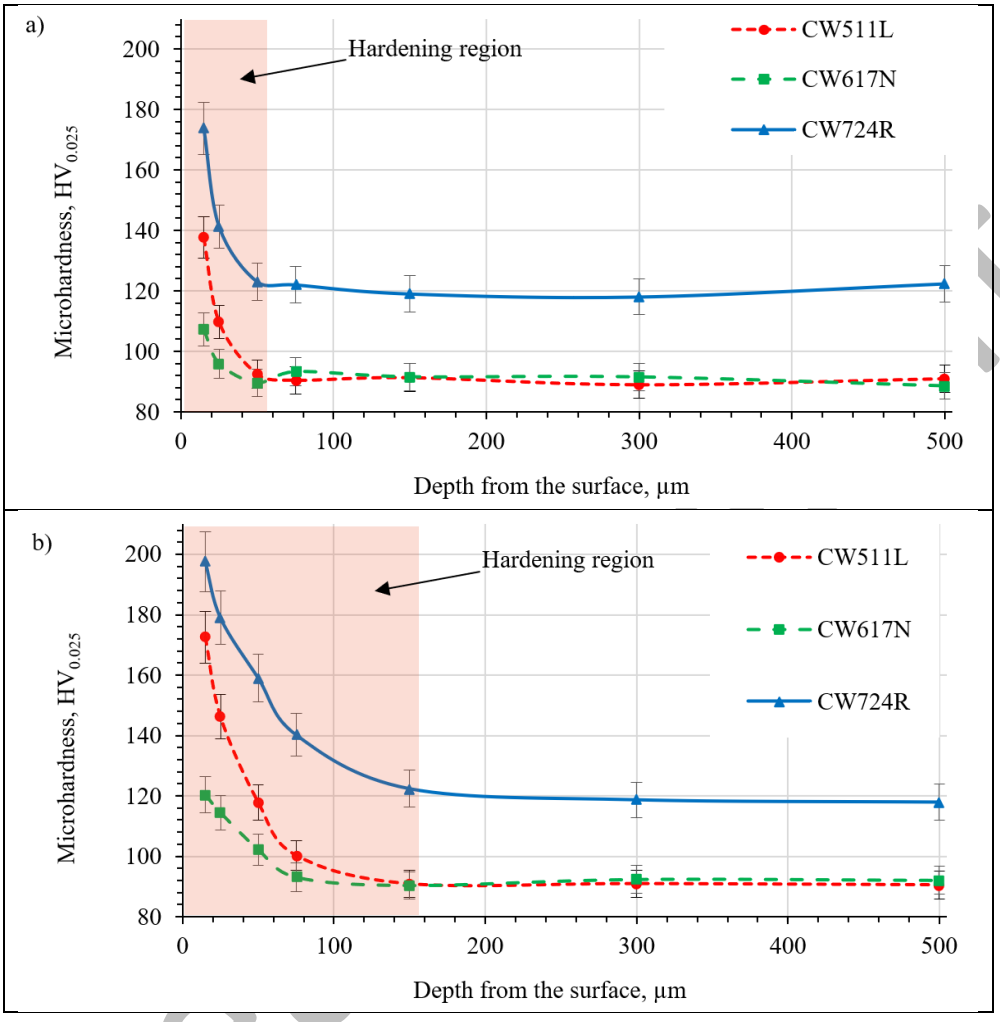

Figure 5. The measured sub-surface microhardness at different depth from the surface; a) ft=0.05, b) ft=0.15 mm/rev.

ENTRY AND EXIT BURR MEASUREMENTS

The specimen is produced during machining operations by eliminating materials until the required shape is achieved. Because of this, cutting-edge technologies are being used in the design and development of high-performance cutting tools. Despite these advancements, there are still certain problems to be solved, such as unwanted burrs. These burrs detract from the assembly's precision, quality, and assembly, and they might also give the operators' hands scratches. The burr creation in a through-the-hole drilling process crops up when the cutting tool enters and exits the workpiece. The burrs at the cutting tool's entrance are the consequence of tool run-out or lateral suppression. However, friction between the cutting tool edges and the workpiece is the main factor contributing to the burr creation at the hole exit [23,27]. The behavior of the materials during plastic deformation, including elongation and fracture, determines the burr height during flat bottom drilling operations. In other words, the production of burrs during machining is an undesirable characteristic linked to the ductility and stresses of the material. The penetrated holes were assessed using four quarter angles of side view photographs in order to determine the burr height, and the average result is shown in Figure 6. Figure 7 illustrates 3D views of the produced burrs near the cutting tool's departure. At a feed of 0.15 mm/rev,

the maximum entrance and exit burr heights for the CW511L are measured to be 0.027 and 0.322 µm, respectively. For CW724R and CW617N, these values are 0.014, 0.086, 0.013, and 0.026 m, respectively. The accordance between the burr height and feed is evident. This can be ascribed to the fact that friction and contact area increase as feed increases, as previously mentioned in this section. Furthermore, compared to CW724R and CW617N, CW511L exhibits a sharper amendment rate of the in both entrance and exit burr height with an increase in feed. This can be attributed to the CW511L's reduced machinability % and increased Pb, Si, and P in its chemical makeup. It is important to note that CW511L, CW724R, and CW617N have respective machinability values of 40%, 80%, and 95%. The main reason for the obtained results is explained in detail in [23].

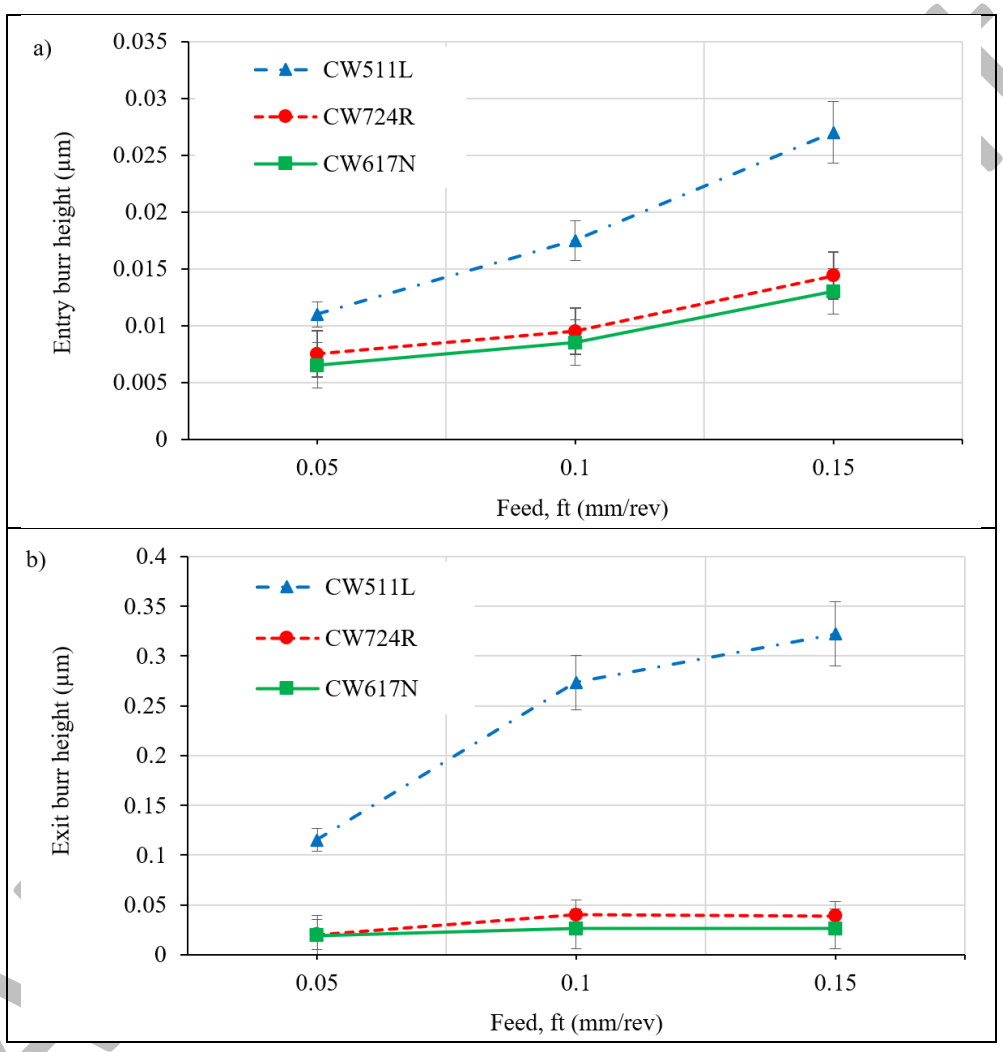

Figure 6. The measured burr height of the drill holes at; a) entry, b) exit.

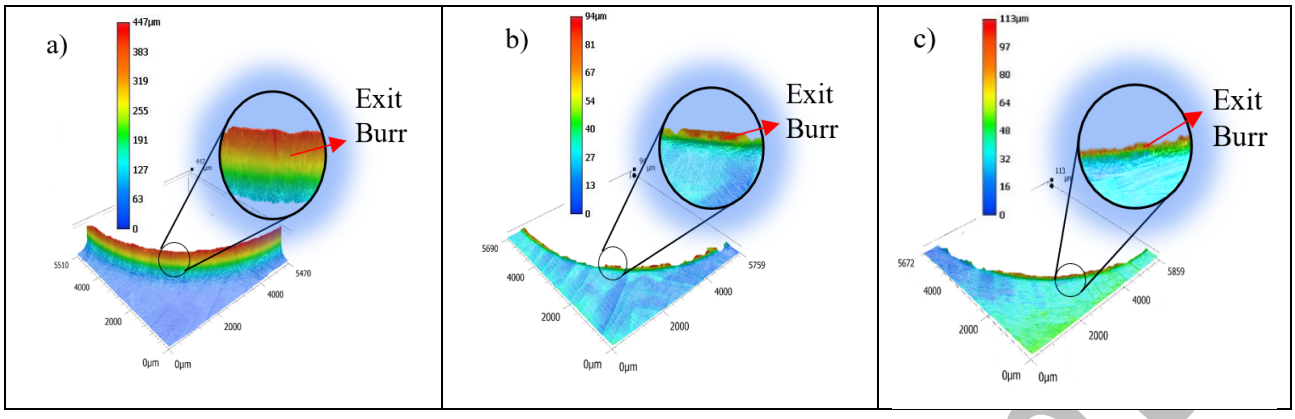

Figure 7. The 3D images of the exit burr; a) CW511L, b) CW617N, c)CW724R

SURFACE MICROSTRUCTURE EVALUATION

The SEM images of lead-free, low-lead, and lead-leaded brass alloys are shown in Figure 8. Images demonstrate that all types of brass include surface flaws, such as deformation and twinning as well as surface and subsurface hardening. Therefore, it can be said that the deformation twinning and an increase in the rate of strain hardening during machining are related. Taking into account the findings from Section 2.2, it was shown that lowering the Pb amount in the alloying composition would result in greater hardness values produced by strain hardening. Additionally, because machining involves a combination of shear, compression, and ductile fracture, the assessment of the surface and sub-surface features must take into account the crystallographic texture. To compare the crystallographic orientation, XRD analysis seems to be necessary for this reason for further studies.

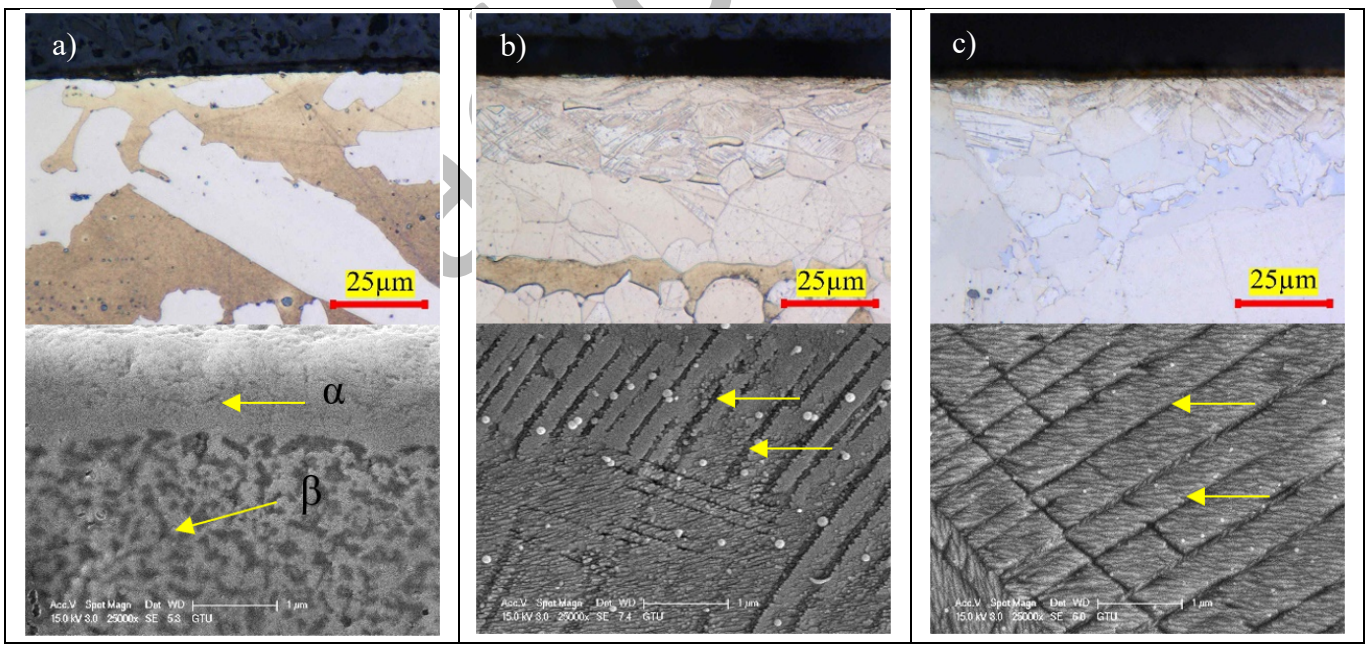

Figure 8. SEM images of the machined surfaces; a) CW617N, b) CW511L, c) CW724R

CONCLUSION

A thorough understanding of the cutting forces, microhardness, surface and subsurface microstructure, and entrance and exit burr formation important to through-all drilling of brass alloys taking the influence of Lead element

was obtained from the research that was conducted. The presence of Pb results in a considerable improvement in chip breakability and a reduction in cutting forces, surface and sub-surface microhardness, and entrance and exit burr development. Leaded brass alloys will generally produce longer chips, greater cutting pressures, increased tool wear, and higher power consumption than low-lead and lead-free brass alloys. Therefore, alternative tools in terms of shape and cutting conditions must be created in comparison to typical leaded ones for the machining of low-lead and lead-free brass alloys. In other words, greater material and machining costs for low-lead and lead-free brasses than for leaded brass will ultimately be inevitable.

Acknowledgements

The authors thank TUBITAK (The Scientific and Technological Research Council of Turkey) for partially supporting this work under project number 118C069.

REFERENCES

[1] Vilarinho, C., Davim, J.P., Soares, D., Castro, F., Barbosa, J. (2005). Influence of the chemical composition on the machinability of brasses. Journal of Materials Processing Technology, 170, 441–447

[2] Szyszkowski, A. (1973). Les principaux laitons au plomb et leurs usages, Centre Belge d' Information du Cuivre. 53, Symposium "Les laitons".

[3] Ragon, R., Stucy, M. (1997). Influence du plomb sur l'usinabilite´ des alliages cuivreux pour robinetterie. Fonderie—Fondeur d' aujourd' hui, 170, 8–15.

[4] Saigal, A., Rohatgi, P. (1996). Machinability of cast lead free yellow brass containing graphite particles. AFS Trans., 104, 225–228.

[5] Whiting, L., Newcombe, P., Sahoo, M. (1995). Casting characteristics of red brass containing bismuth and selenium. AFS Trans., 103, 683–691.

[6] Twarog, D. (1995). Modified red brass with bismuth and selenium: research results. AFS Transactions. 103, 451-461.

[7] L' usinage des alliages cuivreux., 1975, Fonderie—Fondeur d' aujourd' hui, 267, 12–16.

[8] French, A. (1973). Improved free-machining leaded brass. Journal of Institute of Metals. 101, 125–137.

[9] Thomas, P.-J. Le, Arnaud, D. (1959). Influence des impuret´ es sur les proprietes des laitons, Fonderie, 162, 323–325.

[10] https://www.copper.org/applications/rodbar/pdf/A7038-brass-for-european-potable-water-applications.pdf

[11] https://rohs.exemptions.oeko.info/fileadmin/user_upload/RoHS_Pack_9/Exemption_6_c_/Exemption_6c__2015-10-mitsubishi-shindoh-rohs.pdf

[12] Peters, D. (1995). Bismuth Modified Cast Red Brasses to Meet U.S. Drinking Water Standards, Copper Development Association.

[13] Davies, D. (1993) Bismuth in copper and copper base alloys: a literature review. Technical Report, Copper Development Association.

[14] Reddy, V. V., Krishna, A. V., Schultheiss, F., Rosén, B-G. (2017). Surface topography characterization of brass alloys: lead brass (CuZn39Pb3) and lead free brass (CuZn21Si3P). Surface Topograpphy: Metrology, 5

[15] Toulfatzis, A. I., Pantazopoulos, G. A., David, C. N., Sagris, D. S., Paipetis, A. S. (2018). Machinability of Eco-Friendly Lead-Free Brass Alloys: Cutting-Force and Surface-Roughness Optimization. Journal of Metals, 8 (4), 250

[16] Toulfatzis, A., Pantazopoulos, G., Paipetis, A. (2016). Microstructure and properties of lead-free brasses using post-processing heat treatment cycles. Materials Science and Technology, 32, 1771–1781.

[17] Aytekin, K. (2018). Characterization of machinability in lead-free brass alloys, Degree Project In Materials Design And Engineering, Second Cycle, 30 Credits Stockholm, Sweden

[18] Tam, P.L., Schultheiss, F., Sta˚hl, J-E. (2016). Residual stress analysis of machined lead-free and lead-containing brasses. Materials Science and Technology, 32 (17), 1789–1793

[19] Özbey, S. (2020). Production of lead-free brass alloys, and the effect of some additive on machinability, mechanical and corrosion properties. Ph.D. THESIS, Department of Metallurgical and Materials Engineering, Maramara university

[20] Schultheiss, F., Johansson, D., Linde, M., Tam, P.L., Bushlya, V., Zhou, J., Nyborg, L., Ståhl, J.-E. (2016). Machinability of CuZn21Si3P brass. Materials Science and Technology, 32 (17)s, 1744-1750

[21] Johansson, J., Persson, H., Ståhl, J.-E., Zhou, J.-M., Bushlya, V., Schultheiss, F. (2019). Machinability Evaluation of Low-Lead Brass Alloys. Procedia Manufacturing, 38, 1723–1730

[22] Nobel, C., Klocke, F., Lung, D., Wolf, S. (2014). Machinability Enhancement of Lead-Free Brass Alloys. Procedia CIRP, 14, 95 – 100

[23] Zoghipour, N., Tascioglu, E., Kaynak, Y. (2023). Machinability of extruded and multi-directionally hot forged eco-friendly brass alloys. Canadian Metallurgical Quarterly

[24] Zoghipour, N., Tascioglu, E., Atay, G., Kaynak, Y. (2020). Machining-induced surface integrity of holes drilled in lead-free brass alloy. Procedia CIRP, 87, 148-152

[25] Kato, H., Nakata, S., Ikenaga, N., Sugita, H. (2014). Improvement of chip evacuation in drilling of lead-free brass using micro drill, International Journal of Automotive Technology, 8 (6), 874-879.

[26] Fountas, N., Koutsomichalis, A., Kechagias, J.D., Vaxevanidis, N.M. (2019). Multi-response optimization of CuZn39Pb3 brass alloy turning by implementing Grey Wolf algorithm, Frattura ed Integrità Strutturale, 50, 584-594.

[27] https://www.sarbak.com.tr/dokuman/alasimlar/en/